
Modelling Competition for Nutrients between Microbial Populations Growing on Solid Agar Surfaces

Author: Daniel Boocock; Supervisors: Dr Conor Lawless and Dr Paolo Zuliani

October 4, 2016

ABSTRACT

Motivation: Growth rate is a major component of the evolutionary fitness of microbial organisms. When nutrients are plentiful, fast-growing strains come to dominate populations whereas slower-growing strains are wiped out. Maintaining growth rate is therefore a priority for cell lineages and this makes growth rate an excellent surrogate for the health of cells. Measuring the health of cells grown in different genetic backgrounds or environments can inform about genetic interaction and drug sensitivity. In high-throughput procedures such as QFA and SGA, arrays of microbial cultures are grown on solid agar plates and quantitative fitness estimates are determined from growth measurements. Diffusion of nutrients along gradients in nutrient density arising between fast- and slow-growing neighbours is likely to affect growth rate and fitness estimates. However, current analyses assume that cultures grow independently. I study data from QFA experiments growing *Saccharomyces cerevisiae* to test a mass action kinetic model of nutrient dependent growth and diffusion across a network. I try to correct for competition to provide more accurate and precise fitness estimates to allow more accurate and precise genetic interaction and drug screens.

Results: Using far fewer parameters (387 vs 1152), the proposed model fits timecourses from a 384-format QFA plate inoculated with dilute cultures with a similar accuracy to a current QFA model. Accuracy is improved for fast growing strains. Fitness rankings of strains on the same plate agree with a previous QFA study and independent experiments in the positions of the fastest and slowest growing strains, but disagree for medium growing strains. Estimates are less precise for the fastest growing strains, but more precise for 36 out of 50 strains. In cross plate calibration and validation, using QFA plates with a higher inoculum density, the model overcorrects for competition effects to a similar degree that current models undercorrect. A different method of fitting is required to find globally optimal solutions.

Availability and Implementation: CANS, a Python package developed for the analysis in this paper, is freely available at <https://github.com/lwlss/CANS>.

1 INTRODUCTION

The bacterium *Escherichia coli* and yeast *Saccharomyces cerevisiae* are unicellular organisms studied as a model prokaryote and eukaryote respectively. Much of their genomes have been conserved in other species over billions of years of evolution (O'Brien *et al.*, 2005). *S. cerevisiae* was the first eukaryote to have its entire genome sequenced (Goffeau *et al.*, 1996) and is particularly useful as a model of other eukaryotes such

as human cells. Bacteria and yeasts grow in colonies. In favourable conditions, growth is exponential and this makes growth rate a major component of fitness; colonies of faster growing strains quickly come to dominate populations. At a certain point growth becomes limited and a stationary phase is reached so pressure also exists to use resources efficiently. In short, fitness, to a large degree, is governed by competing pressures on growth rate and yield (Dethlefsen and Schmidt, 2007). The growth of microbial organisms can be observed and used to determine fitness estimates (see e.g. Baryshnikova *et al.* (2010a); Addinall *et al.* (2011)). In growth experiments, cell cultures are commonly grown in one of two types of medium: on the surface of a nutrient rich solid agar or in a liquid mixture containing nutrients. In both cases cultures are incubated and cell density is measured over time. Identical strains can grow differently in these environments and disagreement in fitness estimates has been observed (Baryshnikova *et al.*, 2010a). Here, I focus on estimating the fitness of microbes growing on solid agar surfaces.

Fitness estimates can be used to infer genetic interaction or drug response and high-throughput methods allow this to be conducted on a genome-wide scale (see e.g. Costanzo *et al.* (2010); Andrew *et al.* (2013)). In a typical genetic interaction screen a strain is made with a background mutation in a query gene. Double mutants are created by introducing a second deletion to this strain. By comparing the growth of double mutants with controls containing a neutral background mutation (effectively single mutants), genetic interactions can be inferred. If a strain is fitter than predicted given the observation of control fitness, then the deletion is said to suppress the defect of the query mutation. If a strain is less fit than predicted given the observation of control fitness, then the deletion is said to enhance the defect of the query mutation. Either scenario suggests that the two genes interact. Due to redundancy, single deletions are often non-lethal. This allowed Costanzo *et al.* (2010) to explore genetic interactions for ~75% of the *S. cerevisiae* genome.

Synthetic Genetic Array (SGA) and Quantitative Fitness Analysis (QFA) are high-throughput methods for obtaining quantitative fitness estimates for microbial cultures grown on solid agar (Baryshnikova *et al.*, 2010b; Banks *et al.*, 2012). Typically 100s or 1000s of deletions with a common background mutation are pinned or inoculated in a rectangular array on a solid agar plate. Many plates with different query genes and deletions are grown in high-throughput to explore whole genomes. I study data from QFA, which includes quantitative estimation of fitness by measurement and fitting of growth curves. In a typical QFA procedure, liquid cultures are inoculated onto solid agar in a 16x24 rectangular array of

384 spots. Inoculum density can be varied to capture more or less of the growth curve and the most dilute cultures are inoculated with ~ 100 starting cells (Addinall *et al.*, 2011). Plates are grown in a temperature controlled incubator and removed to be photographed periodically throughout the growth curve. Photographs are of whole plates and growth typically covers several days to capture both the exponential and stationary growth phases. Colonyzer (Lawless *et al.*, 2010) processes optical density measurements in photographs to produce a timecourse of cell density estimates for each culture. In past analysis, the logistic growth model was independently fit to the timecourse of each culture and fitness estimates were defined in terms of parameters of this model, namely the growth constant r and carrying capacity K . In contrast, SGA typically uses a larger array of 1536 pinned cultures and a single endpoint assay of culture area to quantify growth. The differential form and solution of the logistic model (Verhulst, 1845) are given in (1), where C represents cell density and $C(0)$ is cell density at time zero.

$$\dot{C} = rC \left(1 - \frac{C}{K}\right) \quad (1a)$$

$$C(t) = \frac{KC(0)e^{rt}}{K + C(0)(e^{rt} - 1)} \quad (1b)$$

The logistic model is a simple mechanistic model describing self-limiting growth and has a sigmoidal solution. Growth begins exponentially with rate rC and curtails as the population size increases and cells begin to compete for some limited resource. Cell density reaches a final carrying capacity K at the stationary phase. In QFA, nutrients must diffuse through agar to reach cells growing on the surface. It is plausible that the carrying capacity K represents the point at which nutrients either run out or growth becomes limited by the diffusion of nutrients and is approximately stationary. Fitting the logistic model to QFA data requires plate level or culture level parameters for $C(0)$ and culture level parameters for r and K making 769 or 1152 parameters per 384 culture plate.

The growth constant r could be used as a fitness measure. However, Addinall *et al.* (2011) define a more complicated fitness measure as the product of Maximum Doubling Rate (MDR) and Maximum Doubling Potential (MDP) which they calculate from logistic model parameters. MDR measures the doubling rate at the beginning of the exponential growth phase, when growth is fastest, and MDP is the number of divisions which a culture undergoes from inoculation to the stationary phase.

$$MDR = \frac{r}{\log\left(\frac{2(K-C(0))}{K-2C(0)}\right)} \quad (2a)$$

$$MDP = \frac{\log\left(\frac{K}{C(0)}\right)}{\log(2)} \quad (2b)$$

To improve the quality of fits, QFA now uses the generalised logistic model which requires an extra shape parameter for each culture (Banks *et al.*, 2012). Standard and generalised logistic model r are not equivalent so comparison relies on

MDR and MDP as fitness measures. The analysis of QFA data using both models is available through the QFA R package (Lawless *et al.*, 2016).

Since QFA aims to determine differences in the fitness of microbial strains from measurements of differences in growth, fast and slow growing cultures are often grown side-by-side. Figure 1 shows a section of a QFA plate from a study by Addinall *et al.* (2011) where this is the case. Cultures were inoculated with approximately equal cell density but have grown at different rates and to visibly different sizes after ~ 2.5 days. Despite starting with the same amount of nutrients and growing at different rates, there is a characteristic timescale for the cessation of growth. This suggests a global growth-limiting effect, which I believe to be caused by an interaction between cultures. I test the hypothesis that the interaction is a competition effect due to the diffusion of nutrients along gradients formed between fast and slow growing neighbours. This has implications for growth estimates; competition will cause growth to appear faster or slower for each neighbour than would be observed if they grew independently. The experiment shown in Figure 2 provides further support for a nutrient competition effect. The same cultures were grown in alternate columns on two separate plates but with cultures added or removed from the neighbouring columns inbetween. Cultures in Figure 2a, where neighbours were removed, grew larger than the same cultures in Figure 2b, where neighbours were added. This suggests that an interaction between neighbours is present and may be affecting fitness estimates. Current QFA analysis using the logistic model assumes that cultures grow independently and ignores possible competition effects between neighbours. The sigmoidal curve of the logistic model poorly fits QFA data in many cases and this may be due to competition effects. I aim to fit a network model of nutrient dependent growth and diffusion to QFA data to try to correct for competition, to increase the accuracy and precision of fitness estimates, and to improve the fit of individual growth curves.

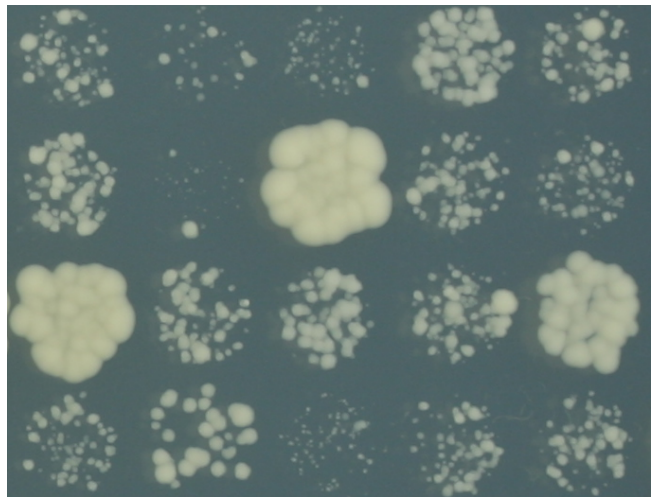


Figure 1: 4x5 section of a QFA plate (P15). Cropped from a 16x24 format solid agar plate inoculated with dilute *S. cerevisiae* cultures. Image captured at ~ 2.5 d after inoculation and incubation at 27°C .

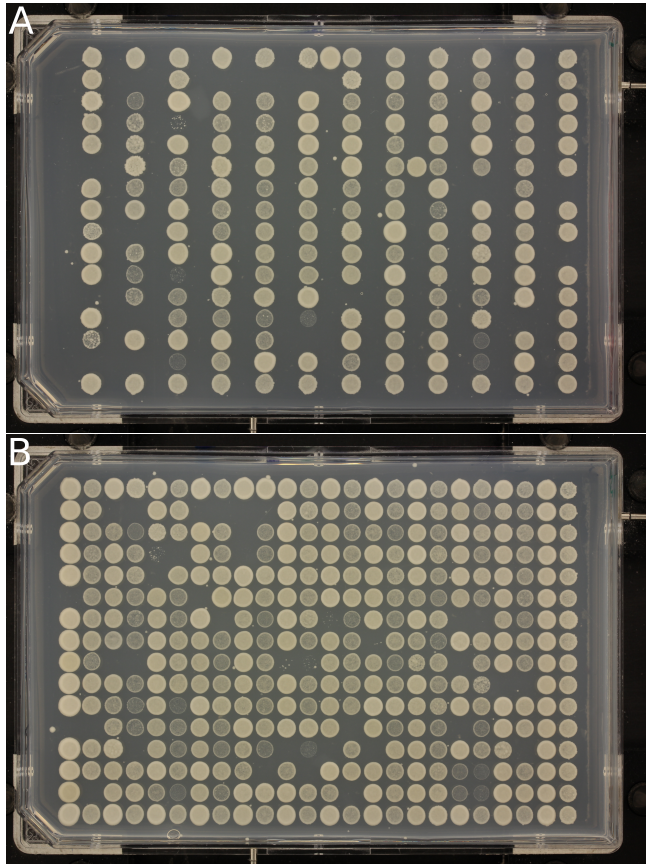


Figure 2: A QFA experiment designed to examine competition.
A) "Stripes" QFA plate inoculated with a more concentrated *S. cerevisiae* inoculum (no cells inoculated on alternate columns). B) "Filled" plate: Same as in A, but with strains of similar growth rate inoculated in the positions missing in A.

Competition effects could be dealt with experimentally by randomising the location of cultures on repeated plates. This does not require explicit knowledge or modelling of the source of interaction but reduces throughput, so, if possible, a modelling approach is desirable. Poisoning of cultures by a signal molecule such as ethanol, which *S. cerevisiae* produces in the metabolism of sugars by fermentation, is another possible source of interaction. QFA does not measure nutrients or signal, so if more than one source of interaction exists, it becomes very difficult to fit a model and randomisation may be the best approach. QFA data for edge cultures is noisy due to reflections from plate edges. This is only partially corrected for by Colonyzer (Lawless *et al.*, 2010) and, as a result, data for edge cultures is usually discarded. Addinall *et al.* (2011) grow repeats of a neutral deletion in edge locations, rather than leaving them empty, because of concerns about competition. In an SGA study, Baryshnikova *et al.* (2010a) use statistical techniques to correct for competition between fast and slow growing neighbours in end-point assays of culture area. I expect that modelling competition for nutrients explicitly will provide a better correction using fewer repeats. QFA uses more information than SGA by fitting whole growth curves, rather than a single endpoint assay, so a modelling approach also promises to be more powerful. Furthermore, modelling may identify and explain the source of competition. Simu-

lations from an accurate model will allow assessment of alternative of experimental designs and prediction of ways to reduce competition effects.

Reo and Korolev (2014) use a diffusion equation model to simulate nutrient dependent growth of a single bacterial culture on a petri dish in two-dimensions. They create a sink for nutrients from culture growth and equate the flux of nutrients through culture area with the rate of increase in culture size. They model culture area as varying and keep culture density constant. This model could be adapted for QFA by approximating culture area as constant and allowing culture density to vary. However, it would be too computationally intensive to fit a similar model to a full QFA plate in three-dimensions, especially if the model is to be used to process many plates from high-throughput experiments. Therefore, a simpler model of nutrient diffusion is required.

Lawless proposed a model of nutrient dependent growth and competition (3,4), hereinafter the competition model, using mass action kinetics and network diffusion (Figure 3). He represents the nutrient dependent division of cells with the reaction equation,

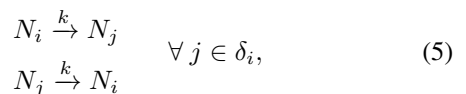


where C is a cell, N is the amount of nutrient required for one cell division, and b is a rate constant for the reaction. (The identity of the limiting nutrient N is unknown but possible candidates are sugar and nitrogen.) He defines separate reactions (3) with growth constant b_i for each culture, indexed i , on a plate and uses mass action kinetics to derive rate equations for the amount of cells and nutrients associated with each culture, C_i and N_i . This gives the rate equation for C_i (4a) and the first term in the rate equation for N_i (4b).

$$\dot{C}_i = b_i N_i C_i, \quad (4a)$$

$$\dot{N}_i = -b_i N_i C_i - k \sum_{j \in \delta_i} (N_i - N_j). \quad (4b)$$

To arrive at the full competition model, he models the diffusion of nutrients along gradients between a culture i and its closest neighbours δ_i by the second term in (4b), where k is a nutrient diffusion constant. This can also be expressed as a series of reversible first-order reactions of the form



and modelled with mass action kinetics. Unlike the logistic model (1), the competition model has no analytical solution, and must instead be solved numerically. If k is set to zero, the competition model reduces to the mass action equivalent of the logistic model, hereinafter the mass-action logistic model, and has the same sigmoidal solution. In this limit, parameters of the competition model can be converted in terms of parameters the logistic model (see Section 2.5). When the competition model is fit to QFA data, C_i is observed and N_i is hidden. Inoculum density, $C(0)$, is often below detectable levels. By assuming that inoculum density is the same for all cultures and that nutrients are distributed evenly throughout

the agar at time zero, initial values of cells and nutrients, $C(0)$ and $N(0)$, can be inferred at the plate level. k is assumed to be constant across the plate but must be inferred. There is a growth constant, b_i , for each of 384 cultures on a typical QFA plate making 387 parameters in total. The competition model shares more information between cultures and has less than half the number of parameters of either the standard or generalised logistic model (Banks *et al.*, 2012; Lawless *et al.*, 2016).

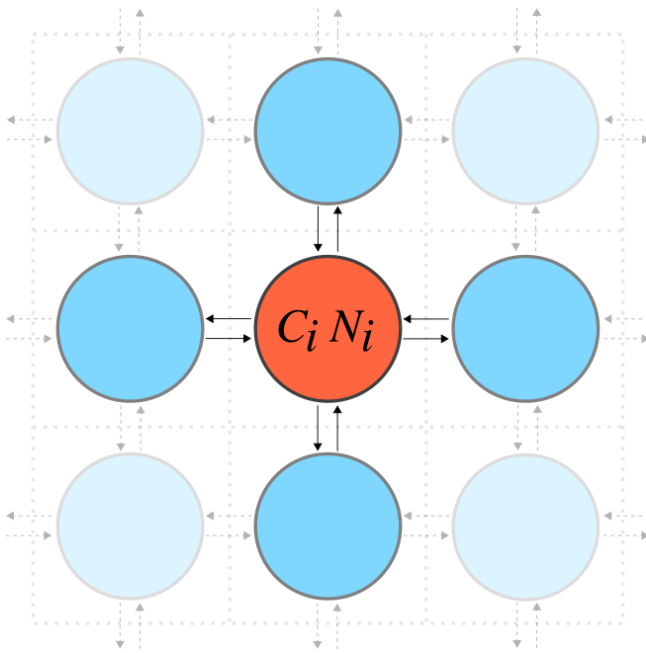


Figure 3: Schematic of the competition model. Each circle represents a culture, indexed i , growing in a rectangular array on the surface of solid agar containing nutrients. Arrows represent a network of nutrient diffusion along gradients between cultures. Darker blue circles δ_i are the closest neighbours of culture i (red).

In QFA, populations begin with ~ 100 cells and quickly grow to reach thousands of cells so the continuum approximation of a deterministic model appears valid. Mass action kinetics applies to reactions in a well stirred mixture and is perhaps less valid for cultures growing on solid agar. However, a mass action approximation has been successful in other situations where this assumption is questionable: in the Lotka-Volterra model of predator-prey dynamics (Berryman, 1992) and in signalling and reaction models inside cells (Aldridge *et al.*, 2006; Chen *et al.*, 2010). The order of a reaction also affects the rate equation, however, the identity and quantity of the nutrient molecule in (3) is unknown. Reaction (3) also assumes that all nutrients are converted to cells and includes no model of metabolism. I justify the use of the competition model because in the independent limit it has the same solution as the logistic model which has long been used to model microbial growth. Furthermore, collectively fitting the competition model involves a large number of parameters and data points and will require many simulations to be run. This necessitates the use of an approximate model for computational feasibility. It is hoped that even an approximate model will be able to more accurately and precisely measure growth parameters

and better estimate fitness. This will increase the power to infer genetic interaction and drug response which could lead to further discoveries. (For an example of a successful QFA study and follow up using the logistic model see Addinall *et al.* (2011) and Holstein *et al.* (2014)).

2 METHODS

2.1 CANS

To analyse QFA data using the competition model I developed the Python package CANS which can be used for model composition, model simulation, parameter inference, and visualisation of results. CANS accepts cell density timecourses for any size rectangular array. CANS can produce SBML models to document results of parameter inference or for independent validation using other simulation tools. It is relatively simple to create and simulate new models involving reactions between species within cultures or between neighbouring cultures, and to fit these provided an initial guess. The CANS package is available at <https://github.com/lwlss/CANS>.

2.2 The P15 dataset

I compared logistic and competition model performance by fitting both models to QFA data for a single plate, “P15” (Figure 1), from a study by Addinall *et al.* (2011). P15 is a 384-culture QFA plate using deletions from plate-15, a standard deletion library in *S. Cerevisiae*, with background mutation *cdc13-1*. *cdc13-1* is a temperature dependent conditional mutatation in a gene involved in telomere stability. Internal cultures consist of 6 repeats of each of 49 different strains with a deletion in a second gene thought to be relevant to telomere function. There are also 14 repeats of a strain with a neutral deletion, *his3Δ*. Edge cultures are also inoculated with repeats of *his3Δ*, but estimates from these cultures are discarded due to noise in cell density estimates caused by reflections from plate walls. Cultures were inoculated with ~ 100 cells which is below levels of detection. P15 was incubated at 27°C , where *cdc13-1* starts to experience loss of function. Each culture has cell density estimates taken at 10 timepoints over 4 days. I elected to study P15 because of the large variation in fitness between strains, which may induce competition effects. There are also many repeats of each strain with which to calculate statistics. Furthermore, independent validation data from spot tests exists in published studies for several strains (Maringele and Lydall, 2002; Zubko *et al.*, 2004; Holstein *et al.*, 2014; Foster *et al.*, 2006).

2.3 The Stripes and Filled plate datasets

The Stripes and Filled plates (Figure 2) are from a QFA experiment designed to study competition (personal communications E. Holstein (April 2016)). On the Stripes plate (Figure 2a), strains are inoculated in every other column, leaving gaps. As for P15 (Section 2.2), strains have a background mutation *cdc13-1* and a deletion in a second gene. There are more strains than for P15 and most cultures have no repeats. The same strains as in the Stripes plate were inoculated in the same positions on the Filled plate (Figure 2b). These were inoculated from the same liquid culture to try to reduce

variation. In the Filled plate, gaps are now filled with new cultures. Each deletion in a new column is a transposition of the strain immediately to the left but with a different background mutation, *rad75Δ*. The left most column is filled with the same neutral deletion, *his3Δ*. The new strains with *rad75Δ* are generally fitter than the common strains with *cdc13-1*. A higher inoculum density ($\sim 10,000$ cells) was used compared to P15 and this was detectable at time zero. Both plates were incubated at 27°C, where *cdc13-1* starts to experience loss of function, and photographed at ~ 50 timepoints over 4 days: around five times more often than for P15.

The experiment is designed to exhibit differences in growth between the same strains on each plate; cultures on the Stripes plate should have access to more nutrients because they grow next to empty locations; cultures on the Filled plate should have access to less nutrients and experience more competition due to the extra neighbours. I used the QFA data from both plates for cross-plate calibration and validation of the competition model by simulating timecourses for the Stripes plate using parameters estimated by fitting the Filled plate.

2.4 Solving and fitting

2.4.1 Solving

CANS numerically solves models using one of two methods. The first is slower and uses SciPy's `integrate.odeint` to solve models written in Python at user supplied timepoints. I vectorised code using NumPy to optimise solving of the competition model by this method. For solving a plate of 384 cultures with cell density observations at 10 unevenly spaced time points, I found that solving time decreased from tenths to hundredths of a second (10 times faster) using the Python bindings for libRoadRunner. libRoadRunner requires models to be written in SBML so I wrote code using the libSBML Python API to automatically generate SBML versions of the competition model for any size plate. Unlike SciPy's `odeint`, libRoadRunner only simulates at uniformly spaced timepoints. To fit QFA cell observations, which are not made at fixed time intervals, requires simulated cell amounts at the observed timepoints. For the analysis of P15, where each timecourse has only 10 timepoints, I simulated sequentially between pairs of timepoints. This method was slower for the analysis of the Stripes and Filled plates where each timecourse had around 50 timepoints. To increase speed, I used SciPy's `interpolate.splrep` to make a 5th order B-spline of cell density timecourses with smoothing condition $s = 1.0$. I evaluated the spline for cell density using SciPy's `interpolate.splev` at 15 evenly spaced timepoints from time zero to the time of the last QFA observation. I then solved these timecourses with one call to RoadRunner.`simulate`.

When using RoadRunner on a modern CPU, fitting a full plate with 10 unevenly spaced timepoints takes ~ 3 hours; fitting a full plate using a spline with 15 timepoints takes ~ 1 hour.

2.4.2 Fitting the competition model

I use QFA data after processing with Colonyzer (Lawless *et al.*, 2010). Colonyzer uses integrated optical density measurements in whole plate images as a proxy for cell density. I used timecourse cell density estimates, which have arbitrary units, throughout my analysis. I fit the competition model using a gradient method and made maximum likelihood estimates of parameters using a normal model of measurement error. For constrained minimisation I used the L-BFGS-B algorithm from SciPy's `integrate` package.

I determined stopping criteria so that parameters of full-plate simulated data sets, with a small amount of simulated noise, were recovered with high precision. To help the minimizer, I scaled $C(0)$ values by a factor of 10^5 to make parameter values closer in order of magnitude. I ran repeated fits using different parameter guesses for each plate (see Sections 3.1 and 3.6). I set bounds according to Table 1 and checked that best fits had no parameters at a boundary.

Table 1: Parameter bounds. Used for fitting the competition model to P15 and the Stripes and Filled plates. Bounds on $N(0)$ were applied to both $N_I(0)$ and $N_E(0)$ for internal and edge cultures. “guess” refers to the initial guess of each parameter (see Section 2.6).

Parameter	Lower Bound	Upper Bound
$C(0)$	guess $\times 10^{-3}$	guess $\times 10^3$
$N(0)$	guess / 2	guess $\times 2$
k	0.0	10.0
b	0.0	None

Cultures at the edge of a plate have an advantage because they have access to a greater area of nutrients. I corrected for this using a separate parameter $N^E(0)$ representing a higher initial amount of nutrients in edge cultures. In rate equations involving edge cultures, I scaled edge culture nutrient amount N_i by the ratio $N^I(0)/N^E(0)$, where $N^I(0)$ is the amount of nutrients in internal cultures. The physical interpretation of this correction is that edge cultures have an extra supply of nutrients that can diffuse instantly into the reaction volume. This treatment reduced the error in cell density estimates for cultures one row or column inside the edge and resulted in better fits to internal cultures overall (see Table 4 in Section 3.4).

Cell density measurements from edge cultures contain more noise due to reflections from plate walls (Lawless *et al.*, 2010). For the competition model, I collectively fit to all cultures and selected best fits based on only the fit to internal cultures.

2.4.3 Fitting the logistic model

Fitting the mass action logistic model requires using culture level $N(0)$ and creating 383 extra parameters. The QFA R package (Lawless *et al.*, 2016) can fit the standard logistic model and has heuristic checks to correct a confounding of parameters that occurs when slow-growing cultures are dominated by noise. I did not have time to implement these checks for the mass action logistic model, so I instead fit using the QFA R package. This is not equivalent because QFA R does not fit data collectively and instead uses a culture level $C(0)$

(1152 total parameters). However, this is a useful comparison with a method of analysis previously used in QFA, including for the analysis of P15 (Addinall *et al.*, 2011). I do not expect much disagreement of fitness estimates with the mass action logistic model once heuristic checks are implemented. In contrast to the competition model, noisy data from edge cultures can be discarded before fitting.

2.4.4 Data visualisation

I created plotting functions in CANS to visualise fits and simulations of QFA timecourses and to compare the ranking of fitness estimates using the Python package matplotlib.

2.5 Parameter conversion

When k is set to zero, the competition model (4) reduces to the mass action logistic model which has the same sigmoidal solution as the standard logistic model. In this limit, it is possible to equate C species of both models and convert parameters using,

$$r_i = b_i(C(0) + N(0)), \quad (6a)$$

$$K = C(0) + N(0). \quad (6b)$$

The reaction equation of the competition model (3) assumes that all nutrients are converted to cells. This implies that all cultures starting with the same amount of nutrients reach the same final amount of cells. Therefore, to fit the mass action logistic model to QFA data, it is necessary to allow $N(0)$ to vary for each culture which is not physically realistic and, in which case, the mass action logistic model has the same number of parameters (769) as the standard logistic model. Figure 4 shows fits of a single culture on a larger 16x24 format plate using both models. This culture grew faster than its neighbours (not shown) and, according to the competition model, competed for more nutrients. Figure 4a shows the mass action logistic model fit where $N(0)$ is estimated as being approximately equal to the final cell amount, or equivalently, carrying capacity K . Figure 4b shows the competition model fit with a plate level $N(0)$ and $k > 0$. Re-simulating with k set to zero gives the dashed mass action logistic model curves which are corrected for competition. We can therefore obtain the corrected logistic model r_i and K_i of these curves by converting from competition model estimates of b_i , $C(0)$, and $N(0)$. N.B. b is the same for both the solid and dashed curves in Figure 4b.

Competition model $C(0)$ and $N(0)$ are the same for all cultures on a plate. Therefore, by the conversion equations (6), all cultures on a plate have the same carrying capacity K and all $b_i \propto r_i$ by the same factor. Similarly, MDP is the same for all cultures and all $b_i \propto MDR_i$ by the same factor (see Equation 2). Therefore, b is equivalent to common QFA fitness measures, r , MDR , and $MDR * MDP$ (see e.g. Addinall *et al.* (2011)). This makes b a very convenient fitness measure for the competition model; we need not convert to logistic model parameters to compare the fitness rankings of cultures on the same plate. To compare competition model fitness rankings between different plates we can of course use b . However, this is not equivalent to comparing r or MDR as different plates may have different $C(0)$ and $N(0)$.

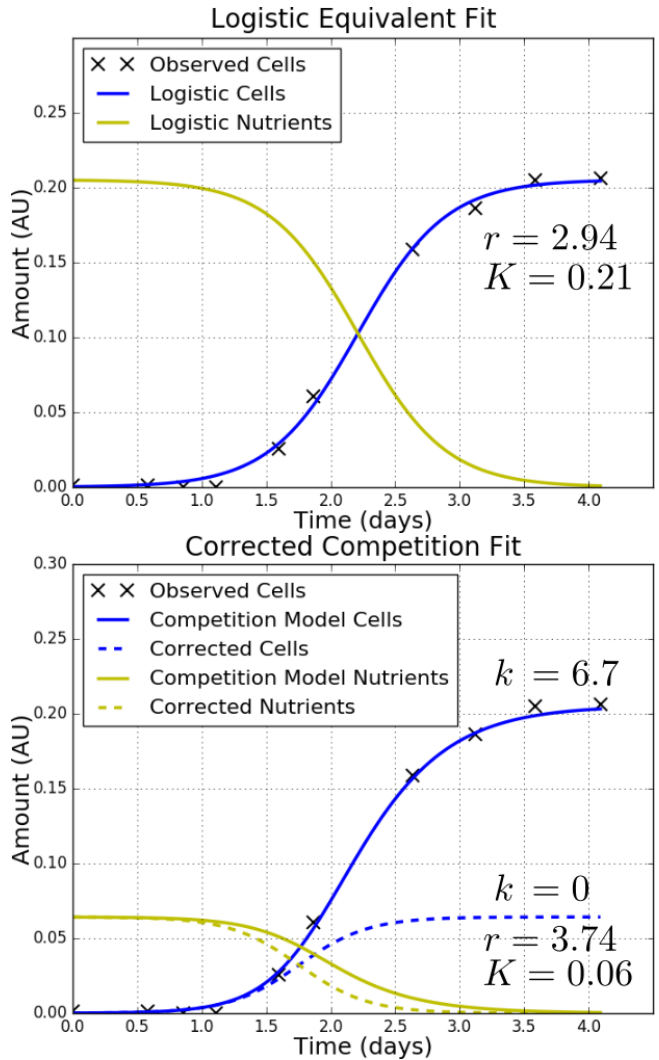


Figure 4: Using the competition model to correct for competition. Fits are to culture (R10, C3) of P15 which grew faster and reached a higher final cell density than its neighbours (not shown). According to the competition model, this is because this culture competed for more nutrients. To reach the same final cell density, the mass action logistic model requires a higher amount of starting nutrients for this culture and a different amount for each neighbour. The correction to the competition model simulates how growth would have appeared without competition and, for the culture shown, gives $r_{\text{corrected}} > r_{\text{logistic}}$ and $K_{\text{corrected}} < K_{\text{logistic}}$.

2.6 Determining initial parameters

Collectively fitting the competition model to a standard 384-format QFA plate is a formidable optimisation problem involving 384 timecourses and 387 parameters. Achieving good fits therefore requires making a good initial guess. To fit small simulated zones I could simply use many random parameter guesses. However, for a full plate the chance of any random guess being close to the “true” values diminishes and more sophisticated guessing methods are required. I developed the *Imaginary Neighbour Model* (Figure 5) for guessing competition model b_i and this allowed good fits of to be made. As the project progressed, it became clear how to convert between fast logistic parameter estimates and com-

petition model parameters (see Section 2.5) and this could be a valid alternative.

2.6.1 Guessing initial amounts

Recall from the competition model reaction equations (3 and 5) that nutrients can only diffuse or be converted to cells. Thus, assuming that reactions are nearly complete at the end of cell observations and that $C(0) \ll C(\infty)$, the total initial amount of nutrients, N_{Tot} , can be estimated using,

$$N_{Tot} = n_I N_I(0) + n_E N_E(0) \approx C_F, \quad (7)$$

where C_F is the total of final cell measurements, n_I and n_E are the numbers of internal and edge cultures, and $N_I(0)$ and $N_E(0)$ are initial nutrient amounts for internal and edge cultures (see Section 2.4.2). Using (7), and an estimate for the ratio of area associated with edge cultures to area associated with internal cultures, $A_r = A_E/A_I = N_E(0)/N_I(0)$, I made guesses of $N_I(0)$ and $N_E(0)$ using,

$$\begin{aligned} N_I(0) &= N_{Tot}/(n_I + n_E A_r) \\ N_E(0) &= N_{Tot}/(n_I/A_r + n_E). \end{aligned} \quad (8)$$

When $A_r = 1$, (8) reduces to the initial nutrient guess for the one initial nutrient parameter model. I used $A_r = 1.5$.

In QFA using dilute cultures, $C(0)$ falls below the level of detection. I did not estimate initial guesses of $C(0)$ and instead ran multiple fits over a range of $C(0)$ values in logspace chosen to encompass uncertainty in $C(0)$ for the given experiment. I expressed this as a ratio, C_r , multiplied by the initial nutrient guess $N(0)_I$.

2.6.2 Guessing b

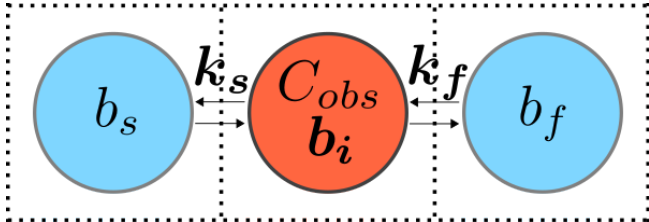


Figure 5: Schematic of the imaginary neighbour model. I developed this model to make quick guesses of competition model b_i by fitting single cultures. A real culture (red) with cell observations, C_{obs} , is modelled as growing alongside imagined slow and fast growing neighbours (blue) with growth constants b_s and b_f (for slow and fast). The model uses separate nutrient diffusion constants k_s and k_f for slow and fast growing neighbours rather than a single parameter k . k_s , k_f , and the growth constant b_i of the real culture are estimated by fitting the model to C_{obs} with all other parameters fixed. Different numbers of each neighbour can be chosen to replicate different configurations of neighbours that might be present on a real plate.

To guess competition model b_i I used the imaginary neighbour model (Figure 5) to quickly fit individual cultures. The model is based on the reaction and rate equations of the competition model (3–5) but tries to replicate the diffusion of nutrients into and out of a culture using imaginary fast and slow growing neighbours, with growth constants b_f and b_s ,

and different nutrient diffusion constants k_f and k_s . To fit the model to QFA data, I fixed $C(0)$ and $N(0)$ for all cultures by the initial guesses (see Section 2.6.1), I fixed b_f at a high value and fixed $b_s = 0$, I allowed b , k_f , and k_s to vary with lower bound zero and no upper bound. I used initial values of zero for k_f and k_s . I carried out multiple fits of the imaginary neighbour model for each value of C_0 , with initial values for b taken from the range (35, 40, ..., 100) and b_f fixed as 1.5 times this value. I determined the number, n , of each neighbour from the guess of $N_I(0)$ and the range of final cell amounts, such that the culture with the highest observed final cell density had enough slow growing neighbours to provide all of the nutrients necessary to reach this final cell density. I solved the imaginary neighbour model using SciPy's odeint and fit using a gradient method as in Section 2.4.2. Fits of the imaginary neighbour model take several minutes which is fast compared to fits of the competition model which take on the order of hours.

2.6.3 Guessing k

Simulations of the competition model using sets of b parameters drawn from different normal distributions have linear relationships between variance in final cell amount and nutrient diffusion constant k . I simulated guessed parameters $C(0)$, $N(0)$, and b_i with a range of different k values and used linear regression to parameterise the straight line. I then took the variance in final cell amount for real data and used the regression model to predict k .

3 RESULTS

3.1 Model comparison using P15

I ran multiple fits of the competition model to P15 (Section 2.2). Each fit used a fit of the imaginary neighbour model (Figure 5) to make initial guesses of b_i . I guessed other parameters as described in Section 2.6 and used separate parameters for the initial amount of nutrients in edge and internal cultures. The imaginary neighbour model itself requires initial parameters and fits looped over combinations of values for initial cell density $C(0)$ and growth constant b . I used five initial values of $C(0)$ ranging from $N(0) \times 10^{-5}$ to $N(0) \times 10^{-3}$ in logspace ($N(0)$ is approximately equal to final cells) and a range of 14 different values for b and b_f as described in Section 2.6.2. This made a total of 70 fits. I show estimated competition model parameters for the top two fits in Table 2. I selected the best fits based on the fit to only internal cultures. Estimated initial nutrient amounts agree fairly well between the top two fits but there is disagreement in estimates of $C(0)$ and nutrient diffusion constant k . It appears that the gradient method is not finding a global minimum. However, b_i estimates were correlated with Spearman's rank correlation coefficient, $\rho_S = 0.989$, and had average mean absolute deviation, $MAD = 1.56$. The mean value of b for the best fit was 44.4 so this disagreement is relatively small.

For all comparisons between the top four fits, ρ_S ranges from 0.922 to 0.995 and b MAD ranges from 1.56 to 6.90. I discarded the 5th best fit, which has less agreement, because, unlike the other fits, it estimated $N_I(0) > N_E(0)$. When comparing this outlier with the top four fits, ρ_S is above 0.930,

but b_i are more affected, with a maximum MAD of 13.29. Despite not finding a global minimum, the best competition model estimates of b_i agree well enough with each to allow meaningful comparison with logistic model parameter estimates.

For the best fit of the competition model to P15 (Figure 9), estimated cell amounts (blue) match the data well across the entire plate. A high nutrient diffusion constant, k , is fit, such that nutrients diffuse readily and nutrient timecourses are similar across local areas of the plate. When comparing objective function values over the plate (Table 3), the logistic model values (smaller) are slightly better. The total objective function value for internal cultures is also slightly better for the logistic model (0.155) compared to the competition model (0.194). However, the logistic model used 1152 parameters to achieve this, whereas the competition model only used 387. The better comparison is with internal cultures because edge cultures have higher noise. To make objective function comparisons fair, I converted logistic model parameters to competition model parameters by (6) and resimulated both models using CANS.

Table 2: Estimated parameter values for the best two competition model fits to P15. Spearman's rank correlation coefficient (ρ_S) between b estimates is 0.989. Mean absolute deviation (MAD) between b estimates is 1.56. The total objective function value for internal cultures is shown in the last column (smaller values are better).

Fit	$C(0)$	$N_I(0)$	$N_E(0)$	k	Obj.
1st	9.1×10^{-5}	0.064	0.090	6.7	0.194
2nd	13.9×10^{-5}	0.062	0.097	8.3	0.196

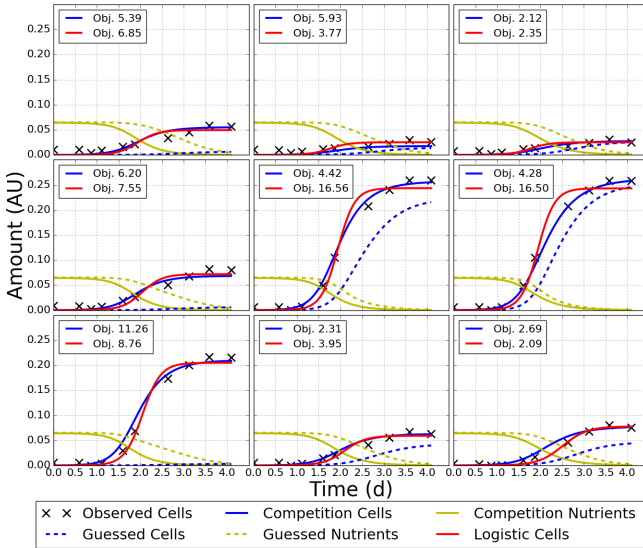


Figure 6: Comparison of competition and logistic model fits to a 3x3 zone of P15. The logistic model (red) was fit with the QFA R package and uses almost three times as many parameters as the competition model (solid lines). The initial guess (dashes) for the competition model was made from fits of the imaginary neighbour model to individual cultures. The zone has top-left coordinates (5, 18) and is boxed in red in Figure 9. Objective function values (Obj.) for each culture were scaled by 10^4 (smaller values are better).

The boxed 3x3 zone in Figure 9 is replotted in Figure 6, with fits of the competition model (solid), imaginary neighbour guess (dashed), and logistic model (red). The zone contains more fast growing cultures than is typical for the plate, so competition effects might be greater than average. The logistic model was fit using the QFA R package (Lawless *et al.*, 2016). The fit of the initial guess is typical for the plate; timecourses for some cultures, such as the bottom-left, are not well fit. However, the guess fulfils its purpose by allowing a good fit to be made when used to initialise parameters of the competition model. The objective function of the logistic and competition model fit is similar for most cultures in the zone. However, for the centre and centre-right fast growing cultures, the competition model has much lower objective function values and appears to fit much better than the logistic model. The total objective function value for the zone is lowest for the competition model: 44.06 vs 68.38 (values scaled by 10^4). The logistic model must provide the better fit for other areas of the plate. Overall, the quality of fit is similar for both models.

Table 3: Objective function values for fits to P15. “Internal” is the total objective function value for cultures not at an edge. “All” is the total objective function value for all cultures on the plate. Smaller values are better.

Cultures	Competition	Logistic
Internal	0.194	0.155
All	0.465	0.345

3.2 Correlation or r estimates between models

To compare model estimates, I converted competition model b_i to logistic model r_i using (6). I took the median r for each deletion for both the competition and logistic model. I took the median, rather than mean, to reduce the effect of outliers that may result from cross-contamination of strains or inoculation of dead cells. Figure 7 shows correlations, between models, of r_i estimates for each culture (black) and of median r estimates for each deletion (red). The distribution for cultures is split into two distinct correlated groups. This is due to a gap in the distribution of logistic model r at around $r = 4$. There is no such gap in the distribution of competition model r . The groups only overlap for medium values of competition model r . The larger group, with lower logistic model r , is correlated with competition model r with gradient close to one. However, competition model estimates were lower for almost all cultures. In the outlying group, competition model r varies more steeply with logistic model r .

There are several extreme outlying cultures (black). The QFA R package uses heuristic checks to correct for confounding between r and K estimates for slow growing cultures. These are required because cultures are fit individually and slow growing cultures contain more noise. For the eight slow growing outliers on the left axis, the checks set $r = 0$. The two outliers with very high logistic r are repeats of $rad50\Delta$ and $est1\Delta$. They have escaped the heuristic checks and exhibit the confounding effect between r and K .

In the distribution of the medians (red), most deletions fall inside the main group of cultures with lower logistic r .

There are also several deletions with high competition model r that fall inside the outlying group (top-right). A significant number of deletions lie in the region between the two groups, meaning that repeats of these cultures are split between the groups. This worsens the correlation of r ranks between deletions compared to cultures. Spearman's rank correlation coefficient, ρ_S , measures the correlation between rank orders of two variables. A monotonic function has a value of 1 or -1. Other correlations fall between these values. For cultures $\rho_S = 0.731$, for deletions $\rho_S = 0.497$.

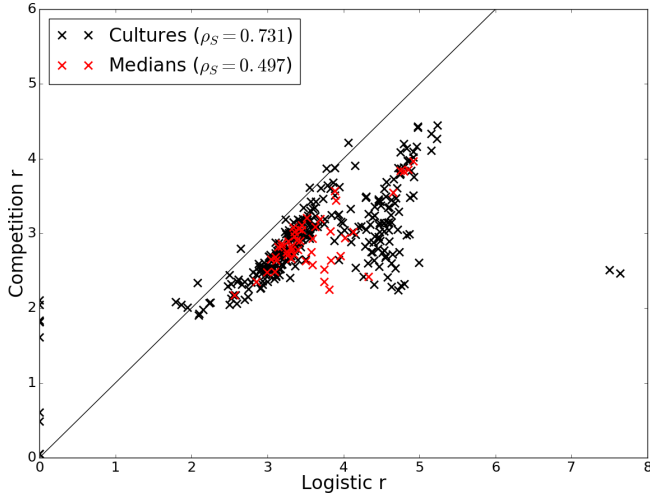


Figure 7: Correlation between logistic and competition model r estimates for P15. Correlations are plotted between r estimates for each culture (black) and between medians of r estimates for each deletion (red). There were six repeats in random locations per deletion (except for the neutral deletion $his3\Delta$ which had 14). Logistic fits used the QFA R package. Spearman's rank correlation coefficient, ρ_S , is shown for each distribution. The line $y = x$ is also plotted.

3.3 Comparison of fitness ranking

In Figure 8, I compare deletions on P15 ranked by competition model b , logistic model r , and logistic model MDR . The fittest deletions are at the top. For each fitness measure, I took the median estimate from repeats of each deletion. I used the QFA R package to infer logistic model r and MDR , and used b from the best fit of the competition model (Section 3.1). Competition model b , r , and MDR rank are equivalent (see Section 2.5) so it is not necessary to convert b to compare rankings.

Logistic model r and MDR rankings agree for all but two deletions: $rad50\Delta$ and $est1\Delta$. These are the same deletions as the two outliers with high logistic model r values in

Figure 7. When MDR is calculated (2a), the confounding between r and K is corrected for and the rank of these deletions agrees well with competition model b rank. As a result, Spearman's ρ_S is higher for competition model b and logistic model MDR (0.635) than it is for competition model b and logistic model r (0.497). When comparing competition model b rank with logistic model MDR rank, there is good agreement between the extreme rankings but middle rankings appear almost inverted. There is also a disagreement of 13 places in the rank of the neutral deletion $his3\Delta$ (bold).

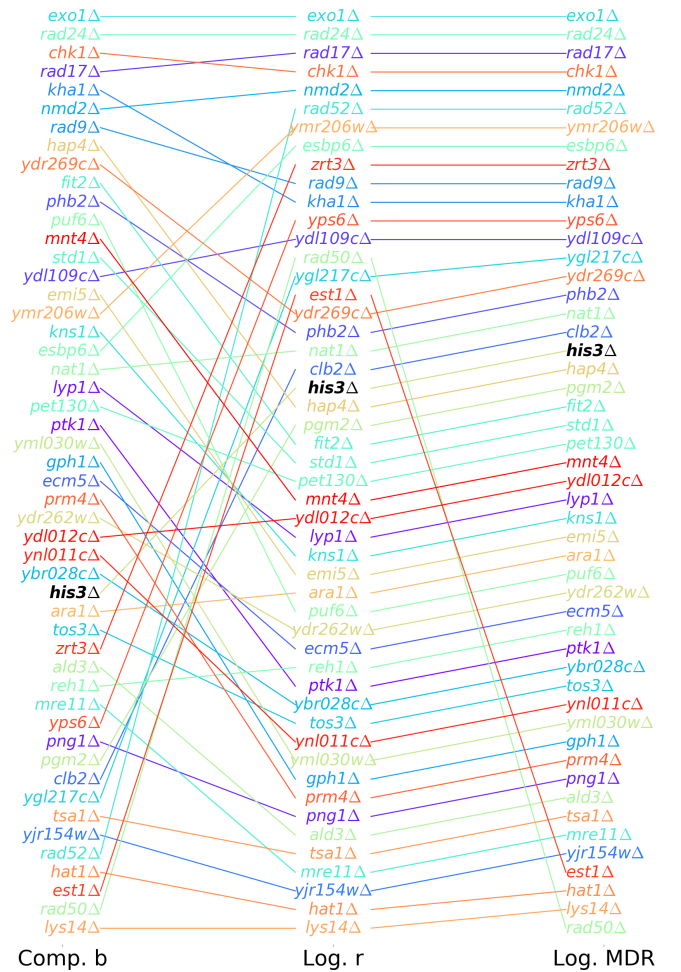


Figure 8: Comparison of fitness ranking for fits of the competition and logistic model to P15. Rankings are determined from median parameter estimates for six repeats of each deletion. Logistic r and MDR were inferred using the QFA R package. For competition b and logistic r , Spearman's $\rho_S = 0.497$; for competition b and logistic MDR , Spearman's $\rho_S = 0.635$. $his3\Delta$ (bold) is a neutral deletion which had 14 replicates.

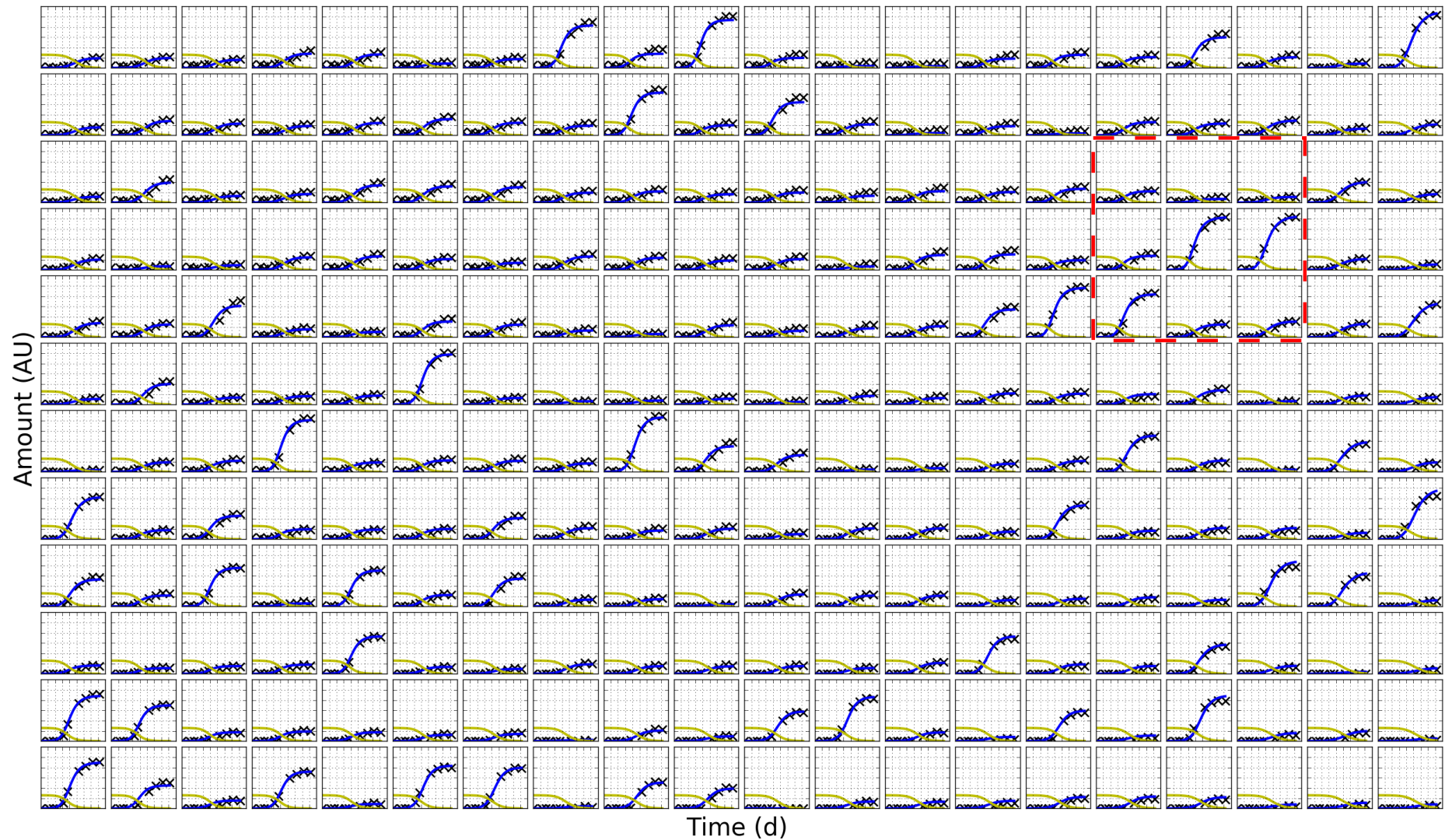


Figure 9: Fit of the competition model to P15. Data is for a 16x24 format plate (P15) with background mutation *cdc13-1* incubated at 27°C. The plate contains 6 repeats of 50 genetic strains randomly arranged across the internal cultures. Repeats of a single strain are used for all edge cultures (removed in the plot). Model output for state variable, cell population size (blue curve), is fit to observed data (black crosses). Model predictions for unobserved variable (nutrient amount) are also plotted (yellow). The outer two rows and columns have been removed. See Figure 6 for a larger plot of the boxed zone.

3.4 Evaluating the treatment of boundaries

I had seen that objective function values were large for edge cultures compared to internal cultures (Table 3). To evaluate the treatment of boundaries, I also fit the one $N(0)$ parameter competition model to P15 using the same method as for the two $N(0)$ parameter model (see Section 3.1). Fits appear similar in quality for both models (Figure 10) and average objective function values for the entire plate are very similar (Table 4). Objective function values for cultures next to an edge culture are improved with the two $N(0)$ model and internal cultures were better fit overall. Interestingly, fits of the edge cultures are actually worse in the two $N(0)$ model. These cultures are dominated by noise due to reflections from plate walls which is why they are discarded from final estimates. However, the edge cultures must be included in the objective function when fitting the competition model. Despite this deficit, the two $N(0)$ model has increased the goodness of fit to internal cultures by collectively fitting all cultures.

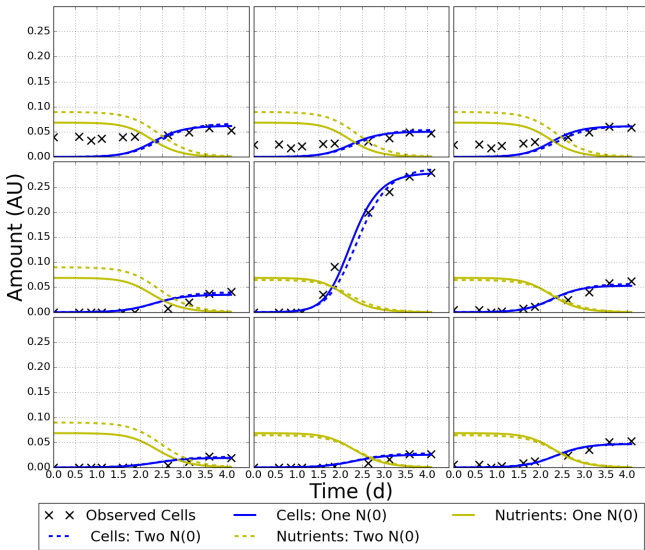


Figure 10: Treatment of boundary conditions in fits of the competition model. The top left corner of a 16x24 QFA plate (P15) fitted with two versions of the competition model: the first with a single initial nutrient amount for all cultures, the second with a separate initial nutrient amount for edge cultures.

Table 4: Average objective function value for one a two $N(0)$ parameter competition models. Values are for the same fits as in Figure 10 and have been scaled by 10^4 . Averages are for cultures belonging to the areas indicated by the column “Cultures”. “Next to edge” refers to cultures one in from the edge. “Internal” refers to all cultures but the edge. Lower values are better.

Cultures	One $N(0)$	Two $N(0)$
Edge	35.9	36.5
Next to edge	9.54	7.98
Internal	6.67	6.30
All	12.4	12.2

3.5 Comparison of Variation in Fitness Estimates

In Figure 11, I compare coefficients of variation (COVs) for competition model estimates of b and logistic model estimates of r between repeats of each deletion on P15. I chose to compare b and r , rather than b and MDR , because both parameters are growth constants in the competition and logistic models respectively. Regardless, COVs for MDR (not shown) are very similar to COVs for r . The precision of fitness estimates is of interest both as a test of the model and because it affects the power to infer genetic interactions. If we assume that biological variation in fitness between repeats of the same strain is small, then the better model should estimate the fitness of strains more precisely, regardless of where repeats are grown on the plate.

Deletions in Figure 11 are arranged from left to right according to competition model b ranking, with the fastest growing deletion on the left. The competition model has a smaller COV for 36 out of 50 deletions. However, the logistic model has a smaller COV for the 11 fastest growers (according to b ranking). Comparing with Figure 7, median values for these deletions (red) appear in the upper right of both groups of cultures (black), not in the gap inbetween. b COV tends to be smaller than r COV at smaller values of b , where repeats are likely to be divided between the groups (as indicated by the positions of medians inbetween groups). The slowest growers tend to have greater COV for both models, which is likely due to the greater effect of noise on cell density estimates in repeats of these deletions.

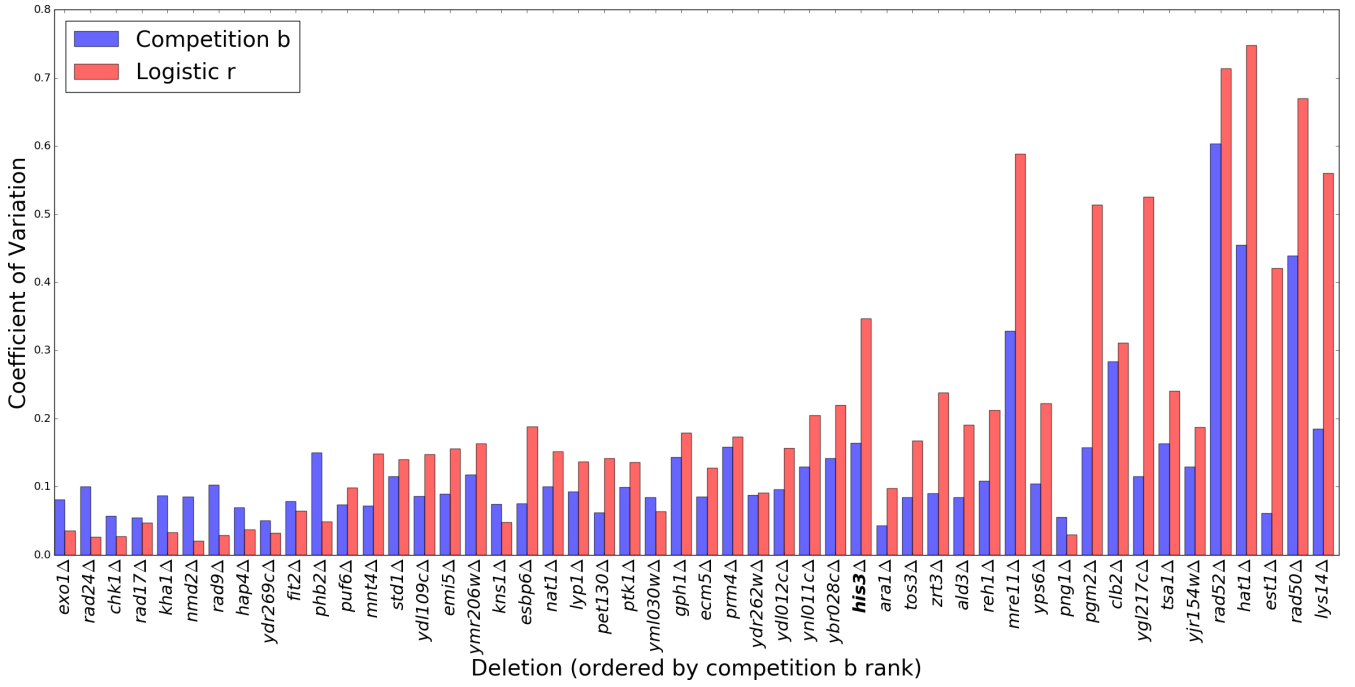


Figure 11: Coefficients of variation (COVs) for growth estimates from P15. COVs are shown for competition model b and logistic model r estimates for repeats of each deletion. COVs of competition model b and r are equivalent (see Section 2.5). Deletions are ordered left to right along the horizontal axis from highest to lowest competition model b ranking. Logistic fits used the QFA R package.

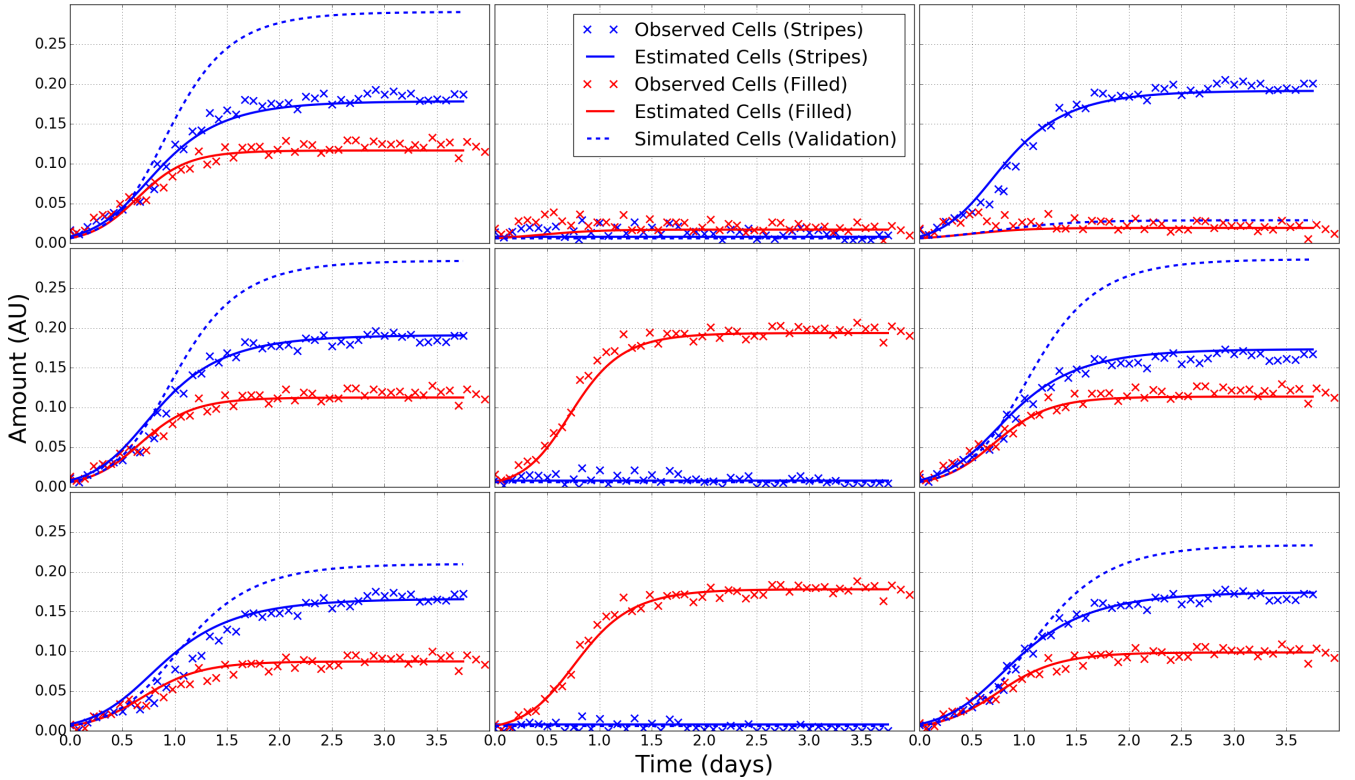


Figure 12: Calibration and validation of the competition model. I fit the competition model to the 16x24 format “Stripes” and “Filled” plates (Section 2.3). The plot shows cell measurements and estimates for both plates for a 3x3 section with top left coordinates (R9, C10). I took the parameters estimates for the “Filled” plate (calibration) and set growth constants, b_i , to zero for cultures in the empty columns of the “Stripes” plate. I then simulated using these parameters to produce the dashed blue curve (validation). If the model corrects for differences in growth between these experimental designs perfectly, the dashed blue curves should resemble the “Stripes” data (blue crosses) in columns one and three. The logistic model would predict no change in growth between plates.

3.6 Cross-plate validation

I used the Stripes and Filled plates experiment (Figure 2) to conduct cross plate calibration and validation of the competition model. As for P15 (Section 3.1), I ran multiple fits of the competition model for each plate. Due to the greater number of timepoints in the data, I fit to cell densities at 15 evenly spaced timepoints taken from a spline of the observed data to increase the speed of fitting (see Section 2.4.1). I used a greater range of $C(0)$ guesses than for P15: 10 values ranging from $N(0) \times 10^{-7}$ to $N(0) \times 10^{-1}$ in logspace. I made this decision due to the higher inoculum densities used in these plates and as a result of discussion with Herrmann and Lawless, who had suggested, based on recent work, that heterogeneity exists within individual cultures such that only a small number of cell lines contribute significantly to final populations. Again, each fit used the imaginary neighbour model to make initial guesses of b_i with 14 different initial b guesses for each $C(0)$ guess (Section 2.6.2). This made a total of 140 fits to each plate. I guessed other parameters as described in Section 2.6 and used separate parameters for the initial amount of nutrients in edge and internal cultures.

The experiment, described in detail in Section 2.3, is designed to test for competition effects. I received the data from E. Holstein (April 2016) in personal communications. The strains in the Stripes plate (Figure 2a) are inoculated in the same positions on the Filled plate (Figure 2b). I took the competition model parameter estimates for the Filled plate and simulated the Stripes plate by setting b to zero for locations in the gaps on this plate. I compared the resulting timecourses with the Stripes cell observations (Figure 12). If the competition model corrects for differences between the plates perfectly, then the simulated timecourses (blue dashes) should fit closely to the Stripes data (blue crosses). I found that the competition model overcorrects for competition; simulated cell densities are higher than observations across the plate. In contrast, the logistic model makes no adjustment between plates and would underestimate observed cell densities by a similar amount. There are some issues with the data set. For instance, the top right culture in Figure 12 does not grow and may have been inoculated with dead cells. However, these mistakes are unlikely to have caused the systematic overcorrection that is observed. Data for empty cultures on the Stripes plate (blue crosses, middle column) is just noise and I excluded these timecourses from the objective function when fitting.

Table 5: Estimated parameter values for the best two competition model fits to P15. Spearman's rank correlation coefficient (ρ_s) for b estimates of the cultures in common is 0.787.

Plate	$C(0)$	$N_I(0)$	$N_E(0)$	k	b (mean)
Stripes	8.3×10^{-3}	0.085	0.096	1.9	39.5
Filled	6.2×10^{-3}	0.116	0.183	4.8	27.9

The inferred parameters for the best competition model fits to both plates are shown in Table 5. Both plates used the same inoculum density and formula of agar so I did not expect plate level parameters to vary between plates. However,

there is significant disagreement in all parameters, indicating that the competition model is not working correctly. There was also more disagreement in the top fits for each plate than was the case for P15, which used a lower inoculum density. Estimates for the five best fits to the Filled plate (Table 5) are only consistent for initial nutrient densities. Despite this, they all overestimated growth when used to simulate the Stripes plate. Disagreement between the best estimates was worse still for the Stripes plate (not shown).

Table 6: Estimated parameter values for the best five competition model fits to the Filled plate. Estimates are ordered by objective function values (Obj.) of the fits where lower values are better. The column MAD b is the mean absolute deviation of growth constants b_i with those of the best fit (row one). Mean b for the best fit was 27.9. Spearman's $\rho_s > 0.96$ for all correlations of these fits.

Obj.	$C(0)$	$N_I(0)$	$N_E(0)$	k	MAD b
0.76	6.2×10^{-3}	0.116	0.183	4.8	-
0.85	5.6×10^{-3}	0.119	0.175	3.1	0.77
0.88	5.0×10^{-3}	0.119	0.175	2.9	1.65
0.93	15.4×10^{-3}	0.114	0.171	4.7	11.1
0.97	3.2×10^{-3}	0.118	0.179	3.8	7.80

3.7 Towards a genetic algorithm

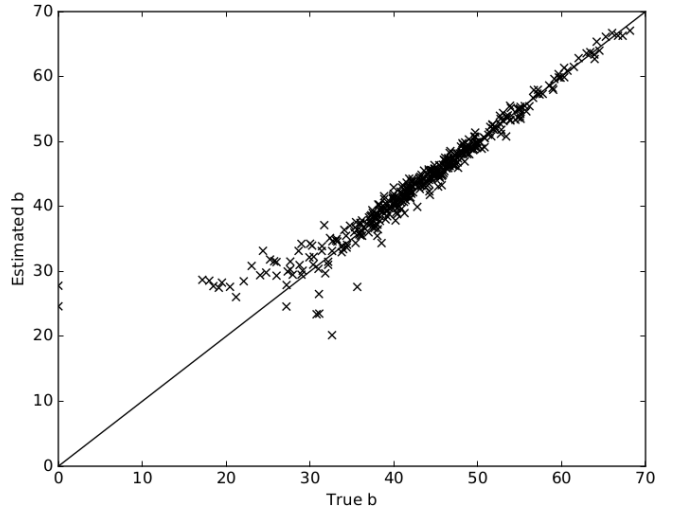


Figure 13: Recovery of true b values from a gradient fit to simulated date using fixed plate level parameters. I simulated timecourses from the best five competition model fits to p15, added a small amount of noise, and used a gradient method to recover b given the true plate level parameters. This plot shows the worst case from the five sets of values.

To test the viability of using a genetic algorithm to evolve plate-level parameter candidates to be evaluated using a gradient method, I took parameter estimates from the five best fits for P15, and simulated full plate timecourses of cell observations with 15 timepoints. I added a small amount of random noise to each timecourse to replicate real data. I then fixed the plate level parameters to the true values and fit the competition model just for b_i . b_i were recovered well even in the worst instance (Figure 13). Estimates are worse for slow growing cultures which are more affected by noise.

4 DISCUSSION

Fits of the competition model (Figures 9 and 6) use less parameters than fits of either the logistic or generalised logistic model from the QFA R package (Lawless *et al.*, 2016). The competition model must also include noisy edge cultures, which contribute disproportionately to the objective function, in collective fits (Section 3.4). Despite this, the fit of the competition model is of similar quality to fit of the logistic model over a whole plate and better in the 3x3 zone studied (Figure 6). In particular, the competition model provided a much better fit to the fast growing cultures in Figure 6. If the source of competition is nutrient diffusion between fast and slow growing cultures, competition effects are likely to be greater for these cultures. The competition model may be correcting for this.

In the correlation of logistic and competition model r estimates for P15 (Figure 7), there is a split in the distribution of logistic model r estimates, but not competition model r estimates. It is possible that the distribution of median r for strains selected by Addinall *et al.* (2011) does have such a split distribution. However, repeats of many individual strains fall in either group but not in the gap. This is evidenced by the positions of medians in the gap (red). It seems unlikely that the same split exists in the distributions of r for repeats of each strain and at the same value. It is possible that the split is either an artefact of the heuristic checks conducted by QFA R fits of the logistic model for slow growing strains (Lawless *et al.*, 2016), or caused by a relative acceleration and deceleration of fast and slow growing cultures due to competition between neighbours. If the latter case is true, the competition model appears to correct for it. It is important to investigate the cause of the split distribution because it will affect the significance given to genetic interactions in QFA studies (see e.g. Addinall *et al.* (2011)).

Competition model ranking of growth estimates for repeats on P15 (see Figure 8) agree with the published logistic model rankings from Addinall *et al.* (2011) for the fastest and slowest growers. Both models also agree with rankings from independent spot tests for these strains (Maringele and Lydall, 2002; Zubko *et al.*, 2004; Holstein *et al.*, 2014; Foster *et al.*, 2006). However, there is much disagreement in the ranking of middle cultures and Spearman's ρ_S for MDR estimates is 0.635. The precision of growth estimates was not improved using the competition model for the fastest growing strains on P15 (see Figure 11). A couple of factors may contribute to this. Firstly, if fast growing cultures are accelerated relative to slower cultures due to competition, this might produce more precise but less accurate logistic model estimates. Secondly, noise dominated cell observations from slow growing cultures will affect collectively fit competition model parameters. This does not affect logistic model estimates because cultures are fit individually. The greater reliability of estimates for slow growing cultures in the competition model could be entirely due to collective fitting rather than to correcting for competition. Although improved, uncertainty in estimates for the slowest growers is still much higher than for the fastest, meaning that the power to infer genetic reactions

would not be dramatically improved.

Fitting the logistic model to slower growing cultures requires heuristic checks to correct for confounding between r and K . The QFA R implementation appears to have some issues. The strains $est1\Delta$ and $rad50\Delta$ are outliers in Figure 7 and this causes a dramatic change in ranking between logistic model r and MDR (Figure 8). I confirmed that these were weak growing strains by visual inspection of the raw QFA images. High r and low K have been erroneously fit to both. This is corrected for when converting to MDR which agrees with the competition model ranking and independent validation for $rad50\Delta$ (Zubko *et al.*, 2004). MDR is more similar to the fitness measure ($MDR \times MDP$) used in the original analysis by Addinall *et al.* (2011) so this is unlikely to have affected their results. For other cultures it appears that encroachment of fast growing cultures into neighbours is affecting cell density estimates made by Colonyzer (Lawless *et al.*, 2010). If repeated, the plate from Addinall *et al.* (2011) should be run with a lower concentration of nutrients in the agar so that the stationary phase is reached before cultures start to merge.

I looked at plate images of P15 to investigate other discrepancies. $hap4\Delta$ appears to be much healthier than $zrt3\Delta$, which agrees with the competition model but not the logistic model (Figure 8). The estimate for $zrt3\Delta$ is more precise for the logistic model than for the competition model (Figure 11). However, this does not confer greater accuracy to either model because the opposite is true for $hap4\Delta$ estimates. Unfortunately, independent data for validation of the middle strains is not available so it is difficult to draw conclusions.

Recent work Herrmann and Lawless suggests that direct measurements of $C(0)$ may not be reliable due to heterogeneity between cells in the same inoculum; many cells do not grow and only the fastest growing cells contribute significantly to the final population. A plate level $C(0)$ also seems inappropriate but having extra parameters for the starting cell density of each culture is undesirable. Only a small amount of nutrients is used when cultures are small. Therefore, early timepoints could be discarded and $C(0)$ could be measured when populations have already undergone several divisions. QFA inocula use cells taken from the stationary phase where there might be more heterogeneity (Bergkessel *et al.*, 2016). It may be possible to increase the precision of fitness estimates by taking inocula from the exponential growth phase or using a higher starting density to average out effects.

The Stripes and Filled plates used a higher inoculum density and had very few noise dominated cultures. Compared to P15, this would have reduced noise in collectively fit competition model estimates and would not have required heuristic checks to be employed for the logistic model. This may therefore be a fairer comparison than P15. It would be informative to repeat P15 with an inoculum density at a detectable level so that the precision of competition and logistic model estimates can be compared in the absence of noise dominated cultures. However the competition model struggled to find a global minimum for the Stripes and Filled plates, which had higher inoculum densities. Therefore, fitting would first

need to be improved. There are issues with validation of both models (Figure 12); the logistic model does not account for differences between plates at all and the competition model overcorrects. As I lack independent data for validation it is difficult to decide which to believe. In any case, it is clear that the competition model could be improved.

4.1 Future work

The split in the distribution of logistic model r (Figure 7) may offer a useful way to compare the logistic and competition models. Firstly, P15 could be repeated using a higher inoculum density to eliminate the possibility that the heuristic checks of the QFA R package are responsible for the split. If the split still exists in only the logistic model, then the strains could be grown in independent conditions, either isolated on solid agar (diffusion still an issue) or in liquid cultures, where the models are equivalent. If the split does not exist in the independent distribution, then we may favour the competition model for QFA plates. This will also depend on how well competition model estimates agree between the two conditions.

I was unable to find global minima using a gradient method to fit the competition model (Sections 3.1 and 3.6). I began work on a genetic algorithm method of solving but lacked time to complete this. I did however find that, with fixed plate level parameters, it is possible to reliably return b_i with a gradient method (Figure 13). This offers the potential to use a hierarchical genetic algorithm where candidate plate level parameters are fixed in gradient fits of culture level parameters b_i . Alternatively, a pure hierarchical genetic algorithm may work (i.e. where b_i are also evolved). A hierarchical Bayesian approach to fitting the competition model, similar to that of Heydari *et al.* (2016), used to fit the logistic model, could also return global minima but might be slow. Current best fits, which are different local minima, have well correlated fitness rankings (Table 6) and make similar over-corrections for competition (Figure 12). This suggests that there is a more fundamental issue with the model.

It would be informative to validate the independent limit of the competition model to determine whether a mass action approximation is valid and whether it is correct to ignore the effect of metabolism on nutrient density. I suggest to validate first in liquid cultures, where the assumption of a well stirred mixture is more valid, and then attempt to validate for single cultures grown on agar, which more closely resembles QFA. Growth on a surface has a lower dimensionality and may be diffusion limited so a fractal kinetics model may be required (Kopelman, 1988; Savageau, 1995). Nutrients (sugars, nitrogen, etc.) in QFA agars are of a standard composition, designed to reduce the excess of any single nutrient (Addinall *et al.*, 2011). It would be helpful to know and control the identity of the limiting nutrient using a different formula of agar. With nitrogen, rather than sugar, as the limiting nutrient, we are less likely to have to model metabolism.

Estimates of the nutrient diffusion constant k were fairly high, such that nutrients diffused readily between neighbours and were nearly depleted when growth stopped. It may be that growth becomes limited by the diffusion of nutrients through

agar before all nutrients are depleted and that nutrients are not well approximated as being evenly distributed across the spatial scales that we model. Using a finer grid could reduce the overcorrection seen in Figure 12. Reo and Korolev (2014) use the diffusion equation with Neumann and Dirichlet boundary conditions to simulate nutrient dependent growth of a single bacterial culture on a petri dish in two-dimensions. They create a sink for nutrients from culture growth and equate the flux of nutrients through culture area with the rate of increase in culture size. They model culture area as varying and keep culture density constant. This model could be adapted for QFA by keeping culture area constant and allowing culture density to vary. A mass action kinetic model of reaction (3) could be used for culture growth and the nutrient sink. It would be computationally challenging to use such a detailed model to fit a whole plate but simulation could be very informative.

If we find that competition for nutrients is not responsible for the interaction between neighbours, for instance if growth becomes limited by diffusion of nutrients in the agar before nutrients from neighbours can be accessed, then we could instead model signalling by ethanol poisoning (Fujita *et al.*, 2006). Signal diffusion may be modelled as we have done for nutrient diffusion (4,5) so much of the code could be reused. If there is any combination of competition, metabolism, signalling, or arrest contributing significantly to differences in the growth of cultures and the interaction between neighbours, then it will be difficult to separate them when fitting a model to data. We may have to develop ways to calibrate effects in isolation and use this information when fitting to high-throughput data. We only have observations for cells.

4.2 Improvements and other recommendations

It is quicker to fit to small zones of a plate but, as these have a larger proportion of edge cultures, boundary conditions become important. Gathering QFA data from smaller arrays grown in isolation would help to speed up the development process.

Each culture is surrounded by a different group of neighbours with different growth constants $b_j \in \delta_i$ (Figure 3). The imaginary neighbour guess (Section 2.6.2) could be improved by using a range of b_f values to fit each culture and selecting b from the best fit. k is the last parameter to be guessed. Rather than using the linear relationship between variance in final cell measurement and k , which may not hold for large values of k , it would be better and just as quick to guess a value of k by fixing all other parameters as the guesses and fitting the competition model to data. It would also be good to compare guesses from the imaginary neighbour model with those from the logistic model. Even with an improved guess, I suspect, based on the closeness of current fits (Figure 6), that a gradient method will still fail to find global minima.

Edge cultures must be included in data when fitting the competition model and this contributed significantly to objective function values (see Table 4). Noise might be better dealt with by leaving edge cultures empty. A different treatment of boundaries could also be used by modelling empty cul-

tures outside edges rather than the approach in Section (2.4.2).

In order to make sure that competition effects were present in data, E. Holstein (personal communications) made a dramatic change between the Stripes and Filled plates. I could have first validated the model against a smaller change, by varying between slower and faster growing cultures rather than no cultures and very strong growing cultures. If the model works well between such plates, it may work well for the majority of QFA experiments which typically have smaller differences between cultures than the data we studied. We could also have calibrated and validated from the Stripes plate to the Filled plate (i.e. in both directions) if the same genotypes had been inoculated in the extra columns of the Filled plate. If we did want to test the an extreme case, we could have inoculated fast growing cultures next to certain strains and not others to try to induce a change in ranking for which the competition model might compensate better than the logistic model.

It is desirable to have a mechanistic model including nutrient dependent growth so that we can use a plate level $N(0)$ and eliminate the dependence on heuristic checks.

REFERENCES

- Addinall, S.G. *et al.* (2011) Quantitative fitness analysis shows that nmd proteins and many other protein complexes suppress or enhance distinct telomere cap defects. *PLoS Genet*, **7**, 4, 1–16.
- Aldridge, B.B. *et al.* (2006) Physicochemical modelling of cell signalling pathways. *Nature cell biology*, **8**, 11, 1195–1203.
- Andrew, E.J. *et al.* (2013) Pentose phosphate pathway function affects tolerance to the g-quadruplex binder tmppyp4. *PLoS ONE*, **8**, 6, 1–10.
- Banks, A. *et al.* (2012) A quantitative fitness analysis workflow. <http://www.jove.com/video/4018/a-quantitative-fitness-analysis-workflow>.
- Baryshnikova, A. *et al.* (2010a) Quantitative analysis of fitness and genetic interactions in yeast on a genome scale. *Nature Methods*, **7**, 12, 1017–24. Copyright - Copyright Nature Publishing Group Dec 2010; Last updated - 2014-09-19.
- Baryshnikova, A. *et al.* (2010b) Synthetic genetic array (sga) analysis in *saccharomyces cerevisiae* and *schizosaccharomyces pombe*. *Methods in enzymology*, **470**, 145–179.
- Bergkessel, M. *et al.* (2016) The physiology of growth arrest: uniting molecular and environmental microbiology. *Nature Reviews Microbiology*, **14**, 9, 549–562.
- Berryman, A.A. (1992) The origins and evolution of predator-prey theory. *Ecology*, **73**, 5, 1530–1535.
- Chen, W.W. *et al.* (2010) Classic and contemporary approaches to modeling biochemical reactions. *Genes & development*, **24**, 17, 1861–1875.
- Costanzo, M. *et al.* (2010) The genetic landscape of a cell. *science*, **327**, 5964, 425–431.
- Dethlefsen, L. and Schmidt, T.M. (2007) Performance of the translational apparatus varies with the ecological strategies of bacteria. *Journal of bacteriology*, **189**, 8, 3237–3245.
- Foster, S.S. *et al.* (2006) Mrx protects telomeric dna at uncapped telomeres of budding yeast cdc13-1 mutants. *DNA repair*, **5**, 7, 840–851.
- Fujita, K. *et al.* (2006) The genome-wide screening of yeast deletion mutants to identify the genes required for tolerance to ethanol and other alcohols. *FEMS yeast research*, **6**, 5, 744–750.
- Goffeau, A. *et al.* (1996) Life with 6000 genes. *Science*, **274**, 5287, 546.
- Heydari, J. *et al.* (2016) Bayesian hierarchical modelling for inferring genetic interactions in yeast. *Journal of the Royal Statistical Society: Series C (Applied Statistics)*, **65**, 3, 367–393.
- Holstein, E.M. *et al.* (2014) Interplay between nonsense-mediated mrna decay and {DNA} damage response pathways reveals that stn1 and ten1 are the key {CST} telomere-cap components. *Cell Reports*, **7**, 4, 1259 – 1269.
- Kopelman, R. (1988) Fractal reaction kinetics. *Science*, **241**, 4873, 1620–1626.
- Lawless, C. *et al.* (2010) Colonyzer: automated quantification of micro-organism growth characteristics on solid agar. *BMC Bioinformatics*, **11**, 1, 1–12.
- Lawless, C. *et al.* (2016) *qfa: Tools for Quantitative Fitness Analysis (QFA) of Arrayed Microbial Cultures Growing on Solid Agar Surfaces*. R package version 0.0-42/r678.
- Maringele, L. and Lydall, D. (2002) Exo1-dependent single-stranded dna at telomeres activates subsets of dna damage and spindle checkpoint pathways in budding yeast yku70 δ mutants. *Genes & development*, **16**, 15, 1919–1933.
- O'Brien, K.P. *et al.* (2005) Inparanoid: a comprehensive database of eukaryotic orthologs. *Nucleic acids research*, **33**, suppl 1, D476–D480.
- Reo, Y.J. and Korolev, K. (2014) Modeling of Nutrient Diffusion and Growth Rate in Bacterial Colonies.
- Savageau, M.A. (1995) Michaelis-menten mechanism reconsidered: implications of fractal kinetics. *Journal of theoretical biology*, **176**, 1, 115–124.
- Verhulst, P. (1845) Recherches mathematiques sur la loi d'accroissement de la population. *Nouveaux memoires de l'Academie Royale des Sciences et Belles-Lettres de Bruxelles*, **18**, 14–54.
- Zubko, M.K. *et al.* (2004) Exo1 and rad24 differentially regulate generation of ssdna at telomeres of *saccharomyces cerevisiae* cdc13-1 mutants. *Genetics*, **168**, 1, 103–115.